Applied Composite Materials
June 2009, Volume 16, Number 3 : Pages 173-182
http://dx.doi.org/10.1007/s10443-009-9085-7

Entire Life Time Monitoring of Filament Wound Composite Cylinders Using Bragg Grating Sensors: I. Adapted Tooling and Instrumented Specimen

H. Hernández-Moreno[1, 2], F. Collombet[1, *], B. Douchin[1], D. Choqueuse[3], P. Davies[3] and J. L. González Velázquez[4]

[1] Université de Toulouse; INSA, UPS; Mines Albi, ISAE; ICA (Institut Clément Ader), 133c, avenue de Rangueil, 31077 Toulouse, France
[2] Instituto Politécnico Nacional, ESIME Unidad Ticomán, Av. Ticomán No. 600, Col. San José Ticomán, 07340 México D. F., México
[3] IFREMER Materials & Structures group, Brest Centre, BP70, 29280 Plouzané, France
[4] Instituto Politécnico Nacional, ESIQIE, Av. IPN s/n, Col. Lindavista, 07300 México D. F., México

*: Corresponding author : F. Collombet, email address : francis.collombet@iut-tlse3.fr

Abstract:

This paper is the first of three describing the monitoring of filament wound cylinders using Bragg grating sensors. Part I describes the technological issues and the development of specimens instrumented with embedded gratings and thermocouples. The aim is to monitor the temperature and strain changes during cylinder manufacture (see Part II) and in-service behaviour (see Part III). Specimens are filament wound glass reinforced epoxy composites, so two technological problems have to be solved: one is to collect data during fabrication and the second is to remove the specimen from the mandrel without damaging the sensors. These were accomplished by design of a specially adapted split mandrel and a rotating interface between the filament winding machine and the composite cylinder in fabrication. Immediately after sensor insertion it was possible to monitor the fabrication process, by collecting Bragg grating wavelength and temperature response, using this specially adapted tooling.

Keywords: Polymer-matrix composites (PMCs) - Residual/internal stress - Non-destructive testing - Filament winding

1. Introduction

Physico-chemical and mechanical studies of cured parts and structures can provide important information on the influence of manufacturing conditions but they are not able to follow the complete history of the fabrication process. Indeed, the severe operating conditions during manufacturing (high temperature, pressure, rotation…) make in-situ measurement recording during the fabrication phase very difficult. The development of optical fibre technologies is one approach to meet this challenge and has been the subject of much recent research activity [1][2][3]. Advantage can be taken of the composite material integration potential, so that composite parts are instrumented with embedded optical fiber Bragg gratings. In the fabrication process of composite cylinders it is of key importance to characterize the material condition during the curing stage, where residual strains are generated. These strains can contribute to defect formation even before service, in the form of internal delaminations [4] and fiber distortion [5]. One way which has been explored for monitoring the material response during fabrication of composite plates is the use of strain and temperature sensors embedded in the material. This in-situ instrumentation could be useful for test-calculation dialogue [6]. The filament winding process is widely used for fabrication of composite cylinders, where the composite cylinder is continuously rotated during both the winding and curing stages, in order to avoid non uniform resin distribution. The rotation makes sensor placement and data acquisition very difficult because the sensors are turning at the same time as the composite component.

In recent years optical fiber based sensors, such as Bragg gratings, have been increasingly used for in situ strain and temperature monitoring, because they produce a minimal host material perturbation [7][2], can be easily embedded [8] and have excellent compatibility with the host [9]. To adapt these fiber sensors to the filament winding process, it is first necessary to develop a technique for placement during winding, and then have an interface between the sensor's wiring (rotating with the component) and the sensor data acquisition instruments, which are stationary and outside the component. There are very few published papers on the monitoring of the fabrication process in filament wound cylinders. Stringer [5] used embedded Bragg gratings for measuring residual strains, before and after fabrication; the main sensors used by Stringer and coworkers, were strain gages and piezo-electric sensors, both embedded. Lee [10] monitored the temperature evolution during curing of composite cylinders made by filament winding, using thermocouples; these specimens were thick cylinders for fly wheel applications. While making measurements, the composite cylinder remained static during curing, so this was not representative of the real filament winding process, where the component rotates. Most of the other published work fielding this area deals with in-service monitoring of composite vessels [11] and risers for the offshore industry [12].

No published papers have been found on the study of strain and temperature monitoring during the fabrication process of rotating filament wound cylinders using fiber optic Bragg gratings. The aim of the present study is to develop a procedure to enable specimens made by filament winding to be instrumented to monitor strain and temperature through the entire fabrication process. This can provide important information for the study of the mechanical response during fabrication, and is important in order to establish the initial material conditions, especially in terms of residual strains (see Part II). In order to position and interrogate this kind of sensor it was necessary to develop an adaptive tooling specially designed for this process. In addition, this allows the optical fiber to be protected after the manufacturing phase, so that measurements can be made during subsequent storage and then throughout the service life as well (see Part III).

2. Fabrication process and cylinder characteristics

2.1. Winding

The filament winding machine used is described in detail elsewhere [13]. Combined axial and rotation displacements produce double helicoidal paths, this kinematic movement forms a rhomboid shaped unit cell, which is a classical filament winding pattern [13]. A detailed explanation of winding patterns can be found in references [14] [15].

2.2. Curing

To maintain a uniform resin distribution, it is necessary to rotate the cylinder during the curing cycle. For this operation a turning mandrel is used, which is placed together with the cylinder in an oven (Figure 1).
The theoretical curing cycle begins with a heating ramp of 3°C per minute for 10 minutes. At 50°C the temperature is kept constant for 900 minutes (due to the temperature tolerance of the prototype rotating connector); the oven cycle finishes with a cooling ramp of 1°C per minute down to 40°C.

2.3. Cylinder dimensions and Materials

The cylinders used in this research were designed as thin walled specimens for external pressure testing in a hyperbaric chamber (see Part III). They have a thickness of 4.42 mm, and the reinforcement fiber is a continuous glass roving (1200 tex), of width 3.5 mm. The winding has a pattern of 1 or 5 rhomboids (2 and 3 specimens respectively) in the circumferential direction. The resin used is a mixture of Araldite LY 5052 and hardener HY 5052. Winding angle is ±55° with respect to the cylinder axis. The number of layers is 7, considering one filament wound layer to be composed of two unidirectional layers, with orientations + α and $-\alpha$. Two zones of reinforcing fibers with an angle of 90° were made at both ends of the cylinder. The final length (350 mm) was obtained by machining the specimen ends, this machining also gave flat end faces to the cylinder, to obtain a hermetic seal for external pressure test (see Part III). The specimen geometry is shown in Figure 2.

3. Adapted tooling

In order to obtain meaningful strain readings with the fiber Bragg grating sensor technique used here, a reference temperature is needed. For this purpose in this work wire thermocouples are used, in addition to the optical fibers. Two optical signal lines, each one having the capability to read several Bragg gratings, and one thermocouple signal line for each optical line were installed in the specimens.
Since both cylinder ends have to be machined and the specimen is to be exposed to external pressure, it is impossible for the embedded sensor's terminals to leave the cylinder through the cylinder end surfaces or by the cylinder external surface. This restriction led to a solution in which the cables exit via the inner surface (compatible with the instrumentation of an autonomous underwater vehicle structure). To

accomplish this, two developments were necessary: first the mandrel design, and second the filament winding machine rotary – static cable interface design.

3.1. Mandrel

A split metallic mandrel design was chosen in order to ensure cylinder dimensional stability, cable passage capability at mid-length, and mandrel extraction without fiber optic damage (see Figure 3).

3.2. Filament winding machine rotary – static cable interface

Because it was desired to have data acquisition during the winding and curing (see Part II), the signal cables (optical and electrical) were placed from the mandrel interior through the filament winding machine hollow spindle shaft and then connected to the interface between static and rotary parts. This was a dual fiber optic rotary joint (FORJ) with an electrical slip ring assembly, both adapted to form a connector system which was installed inside the mandrel (see Figure 4). The system can work in two configurations, one for winding and one for curing. Detailed information can be found in [16]. This system has the capability to acquire data not only during fiber placement and curing (see Part II), but also in service or during mechanical testing to failure (see Part III).

4. Instrumentation characteristics

4.1. Sensor response

Bragg grating sensors for strain measurement are based on wavelength modulation [17]. The Bragg grating has a periodical refraction index variation in the optical fiber core, over a finite length, working as a series of optical mirrors. The refraction index period is called grating period [18]. When the grating is reached by a luminescent signal, the reflected portion has a very narrow band with a central wavelength called the Bragg wavelength λ_B. Temperature variation ΔT, and longitudinal strain ε both produce a wavelength shift $\Delta\lambda_B$ [18] [19]; the simplified grating behavior can be written as equation 1: with $a\lambda_B$, and $b\lambda_B$ being the sensitivities to temperature and strain respectively (see Part II).

$$\frac{\Delta\lambda_B}{\lambda_B} = a\Delta T + b\varepsilon \tag{1}$$

The grating response to hydrostatic pressure is neglected in many applications, since the temperature and strain responses are greater [19] [20], and also because, in this case, Bragg gratings are embedded in the material, so they are sensitive to shell strains and not to hydrostatic pressure. To decouple strain and temperature responses, the thermo-optical sensor response is characterized before the sensor is embedded in the material. Once the thermal response is known, the strain can be obtained if a temperature sensor is embedded just next to the optical grating, in this case this is done with a thermocouple.

The fiber axial strain can be extracted from the absolute wavelength read from the interrogator instrument (*Micron Optics SI 425*), using equation 2 below, where the reading is the Bragg grating wavelength response indicated by the grating interrogator and $\lambda(T)$ is an equation obtained from the grating thermal response characterization, made before sensor placement.

$$\varepsilon = \frac{1}{b\lambda_B}\left[\lambda_{reading} - \lambda(T)\right] \qquad (2)$$

The Bragg grating sensors used in this research have a nominal Bragg wave length between 1530 and 1560 nm. The Bragg grating length is 10 mm and is uniformly inscribed by UV with a phase mask and apodization in a 125 μm diameter optical fiber, having a polyacrylate coating (*SMF-28e*®). It measures a mean strain value over the sensor length. Thermocouples are of K type of diameter 250 μm and with a glass fiber coating. Optical fibers containing Bragg gratings are aligned in both axial and circumferential directions, and a thermocouple is placed next to each Bragg grating.

4.2. Sensor placement technique

Once the conditioned mandrel with the rotary interface and sensors is placed in the filament winding machine (see Figure 5a), the placement of the first epoxy-impregnated glass fibre layer is carried out (Figure 5b), next the sensors are placed over the first layer, one Bragg grating (Fbg1) and one thermocouple (Tc1) in the circumferential direction, and one Bragg grating (Fbg2) and the second thermocouple in the axial direction (Figure 5c). A second layer is carefully wound over the first layer, covering the sensors, and then the rest of the layers are placed as for any other non instrumented specimen (Figure 5d). After curing, the mandrel is carefully extracted from the composite cylinder. The specimen is then ready to follow a machining operation in order to cut the ends, obtain the final dimensions and prepare clean surfaces at both ends (Figure 5e). This results in the finished, instrumented cylinder (Figure 5f).

5. Results and discussion

Several monitoring tests have been performed using the in-situ instrumentation and monitoring technique described here. In each case, wavelength and temperature readings were collected, constituting the raw data, these data were then processed in order to obtain strain and temperature values. The objective of this paper is to demonstrate that the technique functions correctly for monitoring strain and temperature during the fabrication of composite cylinders and also its capability to detect the different events during the filament winding fabrication process. In Figure 6, two graphs are presented, which show the Bragg grating wavelength response together with the thermocouple response. These results are given here as an example of typical curves. Details of these experiments will be presented and discussed in Part II.

The curves in Figure 6 represent wavelength and temperature responses of sensors placed in the circumferential and axial directions of both specimens and are divided into two segments. The first one is the sensor response during winding, and the second segment is the sensor's response during the curing cycle. The time when there is no signal between these segments is the time elapsed while the specimen was transferred from the filament winding machine to the oven, where no data was recorded.

The thermocouple responses show the expected behavior; during winding, the temperature increment with time is due to an increase in ambient temperature. During the polymerization cycle, the temperatures follow the programmed thermal cycle.
The Bragg grating sensors show that the mechanical response of the gratings is negligible compared to the thermal response immediately after insertion. This is because the host material (liquid resin) has no bond with the optical fibers. Once the polymerization has started the matrix begins to form a bond with the optical fiber, and the strain component from the grating signal increases. At the end of the curing cycle, the matrix is completely polymerized and the optical fiber follows matrix strain. In Figure 6, it can be seen that at the end of the curing cycle, the grating response does not reach a value similar to the initial value, while the thermocouple temperature returns to the initial value. This indicates the presence of residual strains; this is clearly observed in the grating in the axial direction. The difference in wavelength values from initial condition to the curing cycle value for gratings placed in the circumferential direction is not significant with respect to the values obtained from axial gratings.
In Figure 6, it may also be noted that during the constant temperature segment of the curing cycle, the circumferential grating response follows the temperature, but in the axial direction, the grating responses change while temperature remains almost constant. A similar behavior of the temperature and grating signal means no change in strain, while any differences between grating signals and thermocouple responses indicate variations in axial strain. At the end of the curing cycle it can be seen that axial grating signals show lower values than those at the beginning of the curing cycle. These represent negative strain (contraction), while in the circumferential direction the gratings have almost the same values as before the curing cycle; there are small positive strain values (which represent a slight expansion).
Specimen strains are obtained by extracting the elastic component from the total grating response, using equation 2. In Figure 7, the axial and circumferential strains plots from the instrumented specimen are shown. These values are obtained substituting the wavelengths and temperatures shown in Figure 6, into equation 2. More detailed results are presented in Part II.
As noted above, during winding, the grating wavelength response follow the temperature variations; this indicates small variations in strains as shown in Figure 7. During the curing stage, the strain variations show clearly that there are residual strains. At the end of the cooling ramp the strain values in the circumferential direction represent expansion, while in the axial direction they represent contraction. The curves in Figure 7 show the strain evolution during the fabrication process, which was the main objective of this research. These graphs demonstrate that the tools designed here and the test procedures are capable of monitoring strain and temperature during composite cylinder fabrication.

6. Conclusion and perspectives

A specially adapted tooling has been developed to collect Bragg grating sensors signals during the filament winding fabrication process, allowing mandrel extraction without optical fiber damage. The integration of Bragg grating sensors during winding and curing is a useful technique for measuring the initial material condition and it was shown that wavelengths can be transformed into strain and temperature. In-situ fiber optic instrumentation was tested and validated and enables the historical evolution of cylinder response during fabrication to be recorded. In Part II, results from tests on five cylinders will show the Bragg grating's capability to monitor strain evolution during fabrication, and their capacity to detect several phenomena occurring during in addition

to quantifying the initial material condition. In Part III, a cylinder previously monitored during fabrication will be tested to failure under external pressure loading, showing the embedded sensor's capability to monitor structural health from fabrication throughout its service life as an underwater pressure vessel.

Acknowledgments

H. Hernández-Moreno wishes to thank the National Council of Science and Technology of Mexico (CONACYT) and the National Polytechnic Institute of Mexico (IPN) for their scholarship sponsorship. The authors thank Messrs. I. Fernandez Hernandez, J. Bauw, F. Afonso, and E. Vargas Rojas for their collaboration during their internship at LGMT.

References

1. Collombet F, Mulle M, Hernandez Moreno H, Zitoune R, Douchin B, Grunevald Y-H. Benefit from embedded sensors to study polymeric composite structures. To be published in Damage and Fracture Mechanics (1st African InterQuadrennial ICF conference AIQ-ICF2008 Algier, Algeria), Boukharouba et al editor, Springer 2008.
2. Sorensen L, Botsis J, Gmür T, Cugnoni J, Delamination detection and characterisation of bridging tractions using long FBG optical sensors, Composites Part A: Applied Science and Manufacturing, 2007/10, Vol. 38, issue 10, p. 2087-2096.
3. Sorensen L, Botsis J, Gmür Th, Humbert L. Bridging tractions in mode I delamination: Measurements and simulations Composites Science and Technology, 2008/12 Vol. 68, Issue 12, p. 2350-2358.
4. Messager T, Pyrz M, Gineste B, Chauchot P. Optimal laminations of thin underwater composite cylindrical vessels. Composite Structures. 2002/12, Vol. 58, Issue 4, p. 529-537.
5. Stringer LG, Hayman RJ, Hinton MJ, Badcock RA, Wisnom MR. Curing stresses in thick polymer composite components. Part II: Management of residual stresses. Proceedings of ICCM-12 Conference. Paris (France), July, 1999. Ref. CD-ROM paper 861, p. 1-10.
6. Collombet F, Mulle M, Grunevald Y-H, Zitoune R. Contribution of Embedded Optical Fiber with Bragg Grating in Composite Structures for Tests-Simulations Dialogue. Mechanics of Advanced Materials and Structures. 2006/08, Vol. 13, Issue 5, p. 429-439.
7. Mulle M, Zitoune R, Collombet F, Olivier P, Grunevald Y-H. Thermal expansion of carbon–epoxy laminates measured with embedded FBGS – Comparison with other experimental techniques and numerical simulation. Composites Part A: Applied Science and Manufacturing. 2007/05, Vol. 38, Issue 5, p. 1414-1424.
8. Ramos C.A., de Oliveira R., Marques A.T. Design of an optical fibre sensor patch for longitudinal strain measurement in structures, Materials and Design, 2008, doi: 10.1016/j.matdes.2008.11.008.
9. Herzberg I, Li H.C.H, Dharmawan F, Mouritz A.P, Nguyen M, Bayandor J. Damage assessment and monitoring of composite ship joins, Composite Structures, 2005/2, Vol. 67, Issue 2, p. 205-216.
10. Lee DH, Kim SK, Lee WI, Ha SK, Tsai SW. Smart cure of thick composite filament wound structures to minimize the development of residual stresses. Comp. Part A 2006/04; Vol. 37, Issue 4, p. 530-537.

11. Degrieck J, De Waele W, Verleysen P. Monitoring of fibre reinforced composites with embedded optical fibre Bragg sensors, with application to filament wound pressure vessels. NDTE Int. 2001/04, Vol. 34, Issue 4, p. 289-296.
12. Brower DV. Structural properties measurements in deepwater oil and gas fields using an advanced fiber optic sensor monitoring system. SAMPE Journal 2005/05, Vol. 41, Issue 5, p. 6-9.
13. Hernández-Moreno H, Douchin B, Collombet F, Choqueuse D, Davies P. Influence of winding pattern on the mechanical behavior of filament wound composite cylinders under external pressure. Composites Science and Technology. 2008/03, Vol. 68, Issues 3-4, p. 1015-1024.
14. Hahn HT, Jensen DW, Claus SJ, Pai, SP, Hipp PA. Structural design criteria for filament-wound composite shells. NASA CR 195125, 1994, p.1-167.
15. Rousseau J, Perreux D, Verdie N. The influence of winding patterns on the damage behaviour of filament-wound pipes. Comp Sci. Tech 1999, Vol. 59, Issue 9, p. 1439-1449.
16. Hernandez-Moreno H, Douchin B, Collombet F, Davies P. Precise positioning of unit cells and embedded instrumentation for fabrication and pressure testing of filament wound tubes. Proceedings of ECCM-11, Rhodes (Greece), May 2004. Ref. CD-ROM 321, p.1-10.
17. Zhou1 G, Sim LM. Damage detection and assessment in fibre-reinforced composite structures with embedded fibre optic sensors-review. Smart Mater. Struct. 2002/06, Vol. 11, Issue 6, p. 925-939.
18. Ferraroa P, De Natale G. On the possible use of optical fiber Bragg gratings as strain sensors for geodynamical monitoring. Opt. Laser Eng. 2002/2-3, Vol. 37, Issues 2-3. p. 115-130.
19. Kang HK, Park JS, Kang DH, Kim CU, Hong CS, Kim C-G. Strain monitoring of a filament wound composite tank using fiber Bragg grating sensors. Smart Mater Struct. 2002/06, Vol. 11, Issue 6, p.848–853.
20. Kuang KSC, Zhang L, Cantwell WJ, Bennion I. Process monitoring of aluminum-foam sandwich structures based on thermoplastic fibre–metal laminates using fibre Bragg gratings. Comp Sci. Tech 2005/3-4, Vol. 65, Issues 3-4, p. 669-676.

Figures

Figure 1. Cylinder installed on the turning mandrel inside the oven for the curing phase.

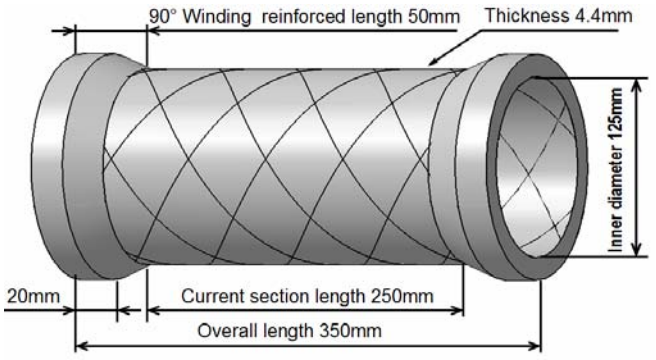

Figure 2. Schematic representation of specimen with dimensions

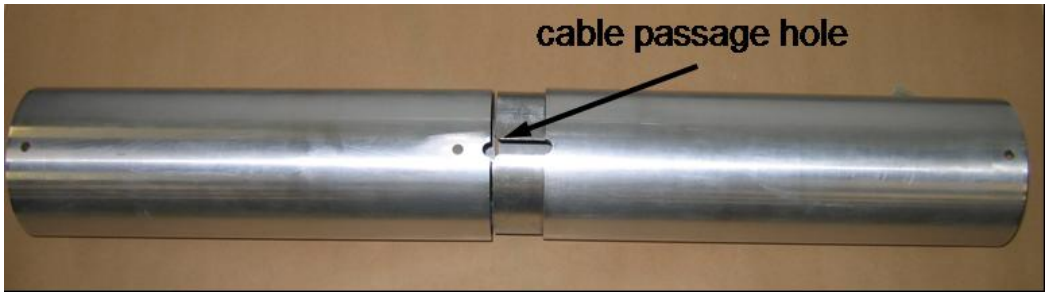

Figure 3. Split mandrel, showing the cable passage and mandrel joint.

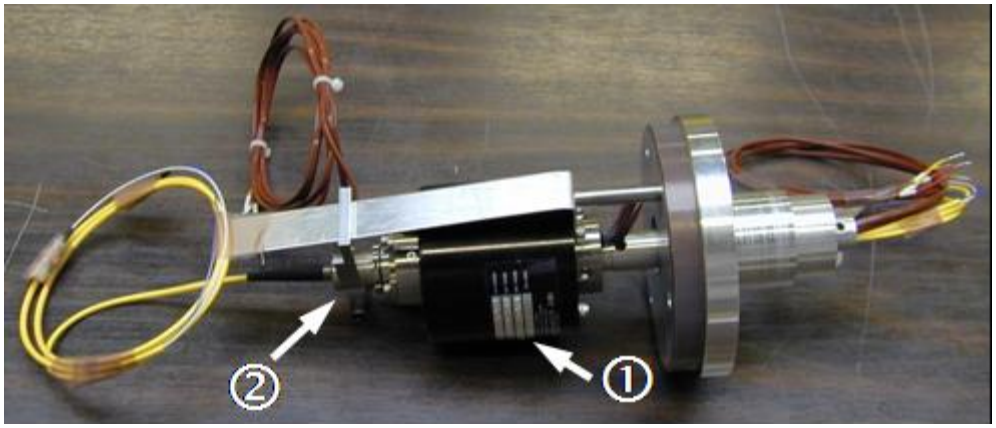

Figure 4. Rotary interface with ① slip ring assembly and ② optical rotary joint.

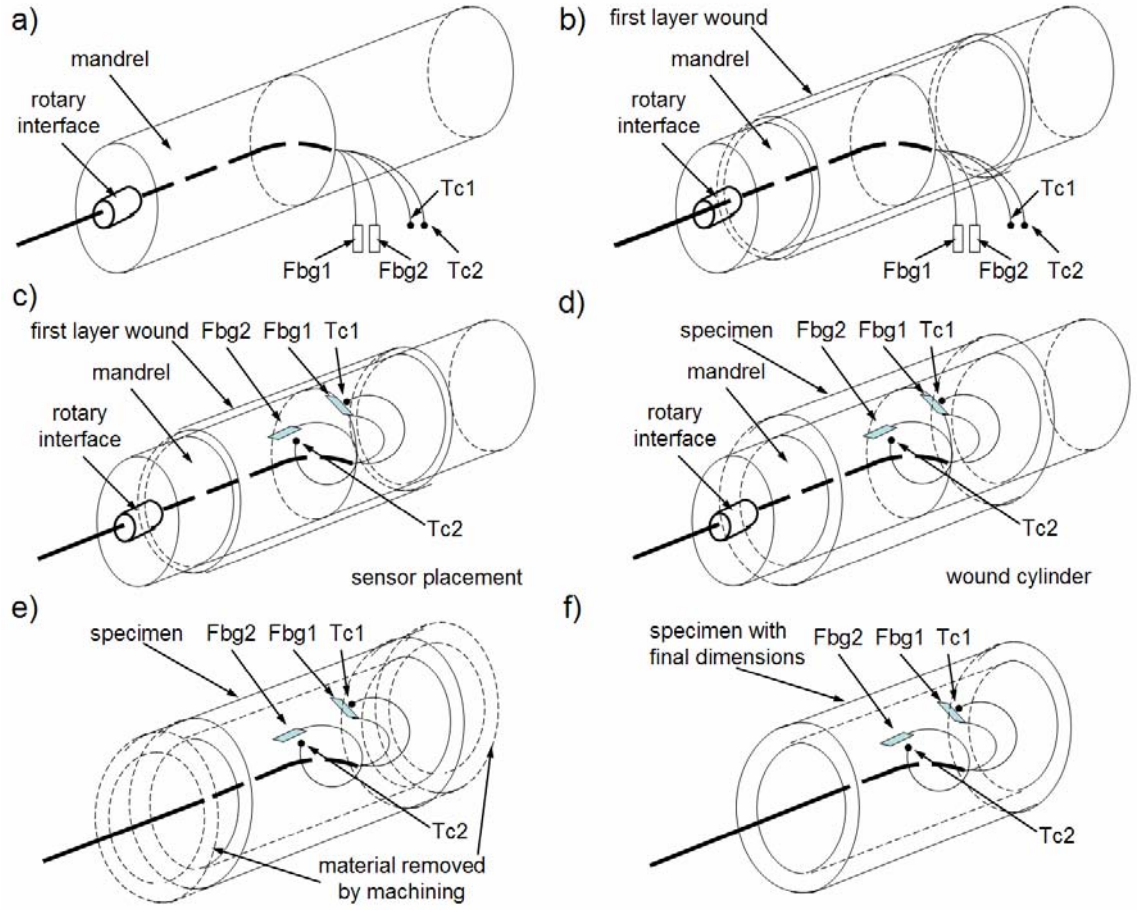

Figure 5. Different steps followed to obtain instrumented specimens with embedded sensors.

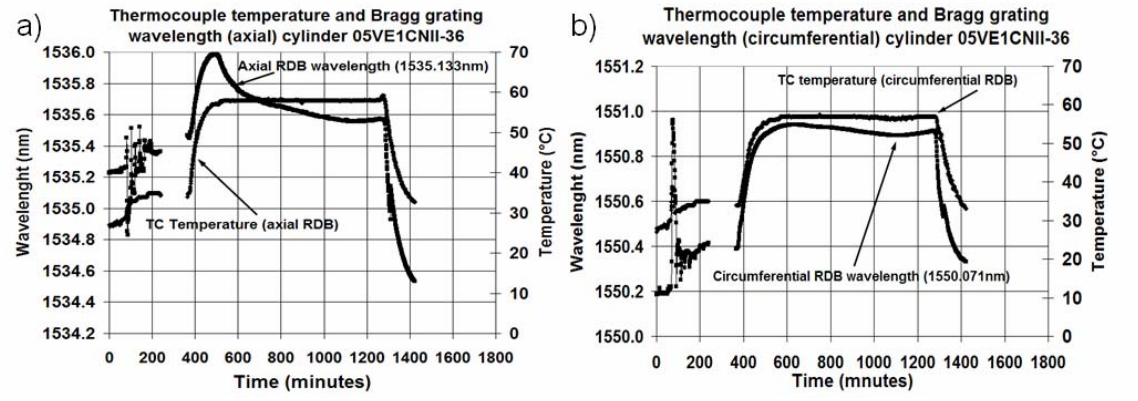

Figure 6. Bragg grating wavelength and temperature responses from instrumented specimen.

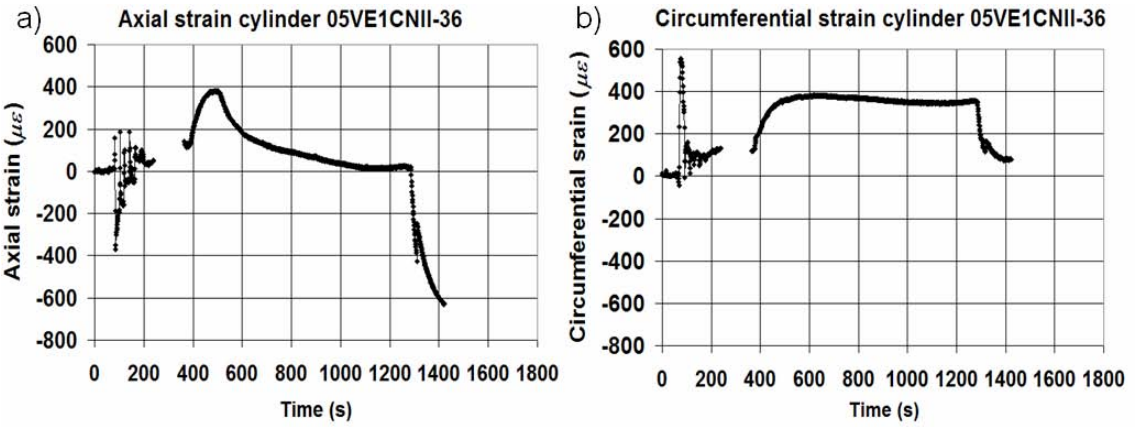

Figure 7. Strain responses from instrumented specimen.